Journal of Environmental Management 342 (2023) 118366

Contents lists available at ScienceDirect

Journal of Environmental Management

journal homepage: www.elsevier.com/locate/jenvman

Research article

# Approach to anaerobic bio-degradation of natural and synthetic fabrics: Physico-chemical study of the alteration processes

Jesús Azcona [a], Catherine Olguín [a], Adrián Durán [a,*], Juana Fernández-Rodríguez [a,b,**]

[a] University of Navarra, Department of Chemistry, Irunlarrea 1, 31008, Pamplona, Spain
[b] University of Cádiz. Department of Environmental Technologies, IVAGRO, Faculty of Marine and Environmental Sciences (CASEM), Pol. Río San Pedro S/n, 11510, Puerto Real, Cádiz, Spain

ARTICLE INFO

*Keywords:*
Anaerobic digestion
Natural and synthetic fabrics
Structural changes
Polymers

ABSTRACT

In this paper, the mesophilic Biochemical Methane Potential of several fabrics was assessed at different Total Solid concentrations (1–4%TS). Physico-chemical techniques were applied to explore the arising structural changes on fibers during the anaerobic digestion process. Additionally, the modified Gompertz model was used to assess and compare the AD performance of the fabrics. In cellulose-based fibers the production of biogas was enhanced thanks to the easy solubilization of acetate, which is generated upon partial breakage of cellulose bonds. The crystallinity of vegetal fibers decreased significantly from day 19. The highest methane yields were attained for silk and wool fabrics at the lowest TS concentrations. Conformational changes in fibroin and keratin were detected. The highest degrees of degradation were observed in solid samples with lower solid concentrations. Accordingly, the maximum methane yields were reported in the reactors operating with lower TS.

## 1. Introduction

Worldwide, 32 kg of textile waste per capita are disposed of each year, of which approximately 87% ends up in landfills (Moazzem et al., 2021). In March 2020, the European Commission adopted a new Action Plan for the Circular Economy, also concerning textile products.

Fabrics aimed at manufacturing clothes and other materials related to the textile sector are made up of fibers. The classification of textile fibers can be summarised into three main groups: natural, artificial and synthetic (Thomas, 2010).

Cellulose is the predominant polymer in cotton, linen and jute, which are vegetal natural fibers; proteins can be found in silk and wool, which are animal natural fibers, and polyester is an example of synthetic fiber. Cotton can be considered as the purest form of cellulose in nature (Hsieh, 2007). Its chemical composition is 85.0–90.0% cellulose, 1.0–3.0% hemicellulose, 0.7–1.6% lignin and 0.8–1.8% pectin. The chemical composition of linen is 85.0% cellulose, 9.0% hemicellulose, 4.0% lignin and 1.8–2.0% pectin. Jute is chemically composed of cellulose (58–63%), hemicellulose (20–24%) and lignin (12–15%) (Ramawat and Ahuja, 2016). Silk is mainly made up of fibroin, which is composed of the amino acids tyrosine, serine, alanine and glycine, forming β-structure (Morton and Hearle, 2008). The silk fibroin is a natural protein with semi crystalline structure, which provides strength to the fiber. Additionally, the sericin acts as an adhesive to hold the structure. Wool is mainly composed of the α-keratin protein (Morton and Hearle, 2008). Polyester is the most commonly used synthetic fibers; its composition is based on an ester of a dihydric alcohol and terephthalic acid.

Anaerobic degradation, happening in the bottom of landfills, can modify the structure of fibers and weaken their bonds within (also forming new compounds), especially those of natural sources. The decomposition process involves the emission of gases, specifically biogas in anaerobic conditions. Sustainable management should be promoted for these substrates. Anaerobic Digestion (AD) could be applied to convert the organic matter of fibers into useful biogas. The microbial processes of AD can be described in sequential process steps: hydrolysis, acidogenesis, acetogenesis, and methanogenesis (Bhatia et al., 2018). As a consequence of the microorganisms' metabolism, the organic matter is converted into biogas, enriched in methane. The most common range of temperatures are: mesophilic (20-45 °C) and thermophilic (>45 °C) (Fernández-Rodríguez et al., 2013; Kothari et al., 2014). The mesophilic range, with an optimal temperature at 35 °C, has shown operational

* Corresponding author.
** Corresponding author. University of Cádiz. Department of Environmental Technologies, IVAGRO, Faculty of Marine and Environmental Sciences (CASEM), Pol. Río San Pedro s/n, 11510 Puerto Real, Cádiz, Spain.
*E-mail addresses:* adrianduran@unav.es (A. Durán), juana.fernandez@uca.es (J. Fernández-Rodríguez).

https://doi.org/10.1016/j.jenvman.2023.118366
Received 28 February 2023; Received in revised form 10 May 2023; Accepted 7 June 2023
Available online 13 June 2023

advantages since the accumulation of inhibitors (as ammonia) is avoided. On the other hand, mesophilic temperatures are more similar to those that can be found in landfills (Fernández-Rodríguez et al., 2010).

Some studies have been carried out involving the AD of textile industry wastewater (Li et al., 2020; Yurtsever et al., 2017). Refractory compounds have also been studied as substrates for the AD process, such as cellulosic materials focusing on improving the methane production (Sasaki et al., 2021). Hamzah et al. (2021) published a review about the valorisation of pineapple waste, a lignocellulosic residue, which involved AD. Cotton wastes are potential substrates for biogas production (Isci and Demirer, 2007; Juanga-Labayen et al., 2020; Binczarski et al., 2022). Nevertheless, the conversion yield of cotton-based textile wastes is very low because of its crystalline structure. Cotton material in combination with paper waste and polyester fraction was tested in mesophilic AD conditions (Juanga-Labayen and Yuan, 2021). In this study, the cotton blend produced the highest biogas and methane yields compared to polycotton. Keratin-rich by-products have also been reported as suitable substrates for AD (Kuzmanova et al., 2018).

X-ray diffraction (XRD) and Fourier Transform Infrared Spectroscopy (FTIR) were employed in the study of cotton stalks, used for biogas production (Zhang et al., 2018). FTIR and SEM (scanning electron microscopy) helped to describe the degradation processes of the cotton stalk and boll (Ghasemian et al., 2016). The changes in lignocellulose biomass from rice straw in the production of biomethane was studied by using XRD and FTIR (Ran et al., 2022), and by XRD, FTIR and thermal analysis (Xia et al., 2018). Rice straw fibers were pretreated with diluted acid and studied by FTIR and SEM (Peng et al., 2019). In the case of the production of biogas with textiles, polyester/cotton were studied after sodium carbonate pretreatment by using SEM and FTIR (Hasanzadeh et al., 2018). The effectiveness of the acid hydrolysis of the cotton fibres wastes was studied by SEM, FTIR and Raman spectroscopy (Binczarski et al., 2022).

In a future practical scenario, this work can contribute to the sustainability of the textile industry. The European principle of Extended Producer Responsibility (OPR) obliges clothing manufacturers to manage waste in a post-consumer stage of a product's life cycle. This study could set the basis for the recovery of textile waste through the anaerobic digestion process, with recovery of useful products such as biogas.

In this work, the AD process of natural and synthetic fabrics was assessed in mesophilic conditions at different concentrations. The monitoring parameters from the process were in liquids, gases and solids substrates, being studied the chemical composition and the structural changes of the solids. The combined use of optical microscopy (OM), colorimetry, FTIR, thermogravimetry (TG) and XRD provides novelty to the study of solid fibers of fabrics under AD. The evolution of the morphology and the colour changes of the fibers, the weakening, breaking and/or formation of bonds, the temperatures of degradation and the modifications in the crystalline structures have been reported.

## 2. Materials and methods

### 2.1. Substrates: textile fabrics and inoculum

The textile fabrics studied in this work were: natural vegetal fibers (cotton, linen and jute), natural animal fibers (silk and wool) and synthetic fibers (polyester). The fabric fibers were acquired in a local fabric store from Pamplona in Spain. The fabrics were cut in squares (size of 4 × 4 cm, approximately). The effluent of a mesophilic reactor from a local wastewater treatment plant (Arazuri WWTP) was used as inoculum.

### 2.2. Experimental system

Biochemical Methane Potential (BMP) assays were carried out in batch reactors (Holliger et al., 2016). In Figure S1 – Supplementary material, a scheme of the experimental set-up can be observed, similar to De Diego-Díaz et al., 2019. The reactors were made of polyvinyl chloride (PVC) with 5.0 $L_{total\ volume}$ and 3.0 $L_{working\ volume}$. The reactors were placed in a closed thermostatic chamber with a constant temperature of 35 ± 1 °C. Wet range was chosen and the inoculum supposed 1/4 of the working volume (0.75 L). The inoculum to substrate ratio (I/S) was in the range 0.3–1.3 (Table 1), since previous studies reported that 0.6 approx. was the ratio for the maximum methane yield in the Anaerobic Codigestion (AcoD) of Food Waste (FW) and sludge (Johnravindar et al., 2023). Synthetic wastewater with a relationship of C/N/P 100/10/2 used in previous literature (Wang et al., 2016; Villain et al., 2014) was prepared to feed the reactors (2.25 L/reactor) (Table S1-Supplementary material). The synthetic wastewater supplied, in a balanced composition, the nutritional support to the anaerobic microorganisms. In the batch reactors, the solid fabrics under different concentrations (TS%) were added as well as the inoculum and the water. Table 1 summarize-up the experimental set-up.

### 2.3. Analytical methods

The samples: liquid, gas and solid; were collected from the batch reactors on different days (0, 3, 11, 19, 30 and 40).

2.3.1. Liquid samples: The analytical methods for quantification of pH, soluble Chemical Oxygen Demand ($COD_s$), Total Organic Carbon (TOC) and Dissolved Organic Carbon (DOC) in liquid samples were carried out according to standardized methods (APHA/AWWA/WPCF, 2012; De Diego-Díaz et al., 2019).

2.3.2. Gas samples: The biogas production was determined by bubbling it through a gasometer and $CH_4$ content was analysed with a gasometer containing an alkaline solution (Holliger et al., 2016; De Diego-Díaz et al., 2019). Additionally, a biogas analyzer (Geotech Biogas5000) was used to quantify the composition of biogas.

2.3.3. Solid samples of fiber fabrics: FTIR, XRD, thermal analysis and optical microscopy were employed as in previous papers (De Diego-Díaz et al., 2019; Olguin et al., 2022). For the cellulose-based fibers, two ratios were considered in FTIR: acetate content = $I_{1540}/I_{1635}$ (Eq. 1); and amorphous content = $I_{1335}/I_{1314}$ (Eq. 2). In the case of the protein-based fibers, amino acid content in silk = $I_{1002}/I_{3284}$ (Eq. 3) and degree of degradation (peptide bond hydrolysis) = $I_{1626}/I_{1516}$ (Eq. 4). The crystallinity of the cellulose fibers was estimated by using CrI = $(1 - \frac{I_{am}}{I_{002}})\cdot 100$ (Eq. 5) in XRD. The CIEL*a*b* colorimetry experiments were performed by triplicate using a KONICA MINOLTA Spectrophotometer CM-2300 d with light D65.

### 2.4. Kinetic analysis

The methane production kinetic was modelled through modified Gompertz model based on (Zwietering et al., 1990), since the methane production would correspond to methanogenic population growth. Several studies about AD of fibers were fitted to Gompertz model, as cotton (Juanga-Labayen and Yuan, 2021) or cellulose-based substrates (Krungkaew et al., 2022; Ebrahimzade et al., 2022; Ziemiński and Kowalska-Wentel, 2015). The modified Gompertz equation as follows:

$$y(t) = y_m \cdot \exp\left\{ -\exp\left[\frac{R_{max.}}{y_m} e \cdot (\lambda - t) + 1\right]\right\} \quad \text{(Eq. 6)}$$

where.

$y(t)$ is the cumulative methane yield (L/kg) at a time t (days).

$R_{max.}$ is the maximum specific methane production rate (L/(kg-VS. day))

$y_m$ is the maximum methane yield potential (L/kg-VS).

$\lambda$ is the lag-phase time (days).

$e$ is a mathematical constant (2.71828).

**Table 1**
Description of the experimental set-up.

| Textile fabric | | | TS (%) | Nomenclature | Fabric mass (g) | Inoculum (L) | I/S ratio | Synthetic wastewater (L) |
|---|---|---|---|---|---|---|---|---|
| Blank | | | 0 | B | 0 | 0.75 | – | 2.25 |
| Natural | Vegetal (cellulose-based) | Cotton | 4 | C4 | 120 | 0.75 | 0.3 | 2.25 |
| | | | 2 | C2 | 60 | 0.75 | 0.6 | 2.25 |
| | | Linen | 4 | L4 | 120 | 0.75 | 0.3 | 2.25 |
| | | | 2 | L2 | 60 | 0.75 | 0.6 | 2.25 |
| | | Jute | 4 | J4 | 120 | 0.75 | 0.3 | 2.25 |
| | | | 2 | J2 | 60 | 0.75 | 0.6 | 2.25 |
| | Animal (protein-based) | Silk | 2 | S2 | 60 | 0.75 | 0.6 | 2.25 |
| | | | 1 | S1 | 30 | 0.75 | 1.3 | 2.25 |
| | | Wool | 2 | W2 | 60 | 0.75 | 0.6 | 2.25 |
| | | | 1 | W1 | 30 | 0.75 | 1.3 | 2.25 |
| Synthetic | | Polyester | 2 | P2 | 60 | 0.75 | 0.6 | 2.25 |
| | | | 1 | P1 | 30 | 0.75 | 1.3 | 2.25 |

## 3. Results and discussion

### 3.1. Cellulose-based fabrics

The highest values of biogas production were found on day 14 in reactors with cotton, linen and jute, which corresponded to the hydrolytic and acidogenic stages. The methane composition was located in the range 74–76 ± 4% in the reactors (Table 2). From day 14, biogas production began to drop, until a plateau was reached from day 21 (Fig. 1a and 1b). The highest values of biogas production were found in reactors with the lower solid concentrations (C2 and J2) except for linen. In this case, L4 showed the highest value of daily biogas production, ca. 1.2 L, at 14 days (Figs. 1a) and 12.2 L of accumulated biogas (Fig. 1b). In some fabrics -L2, J4-, an increment in biogas could be reported in the last days of experimentation, 37–40 days. Those increments are consistent with acetate content in the material (Fig. 1d).

pH was measured to maintain an optimal state for methanogenic microorganisms' action. NaOH was added in order to maintain the pH values around 7.5 (Lee et al., 2009). However, acidification was reported in all the cellulosic reactors until day 11 (Fig. 1c), due to the hydrolytic and acidogenic phases in which Volatile Fatty Acids (VFA) were released. During the acetogenesis step, these VFA were consumed, and pH values increased (Jeihanipour et al., 2013). The pH decreases average in the three fibers types from 0 to 11 day was 25.3%, being maximum in linen and cotton (30%) and minimum in jute (12%). The higher concentration of non-inhibitory VFA can be related to the maximum production of biogas in the system, which would justify the performance of L4. In this system, the pH was lower than other conditions during the first 30 days, reaching the methanogens optimal pH at the end of the assay. From day 11, the pH values began to increase between 6.5 and 7.5, which were optimal values for the biomethanization process.

The data obtained of biogas production and pH, which indicated the beginning of the acetogenic phase in the day 11, clearly matched those from the IR spectra of cotton, linen and jute. From day 11, two bands appeared in the spectra of solid fibers at 1540 and 1390 $cm^{-1}$ (Fig. 2). These bands may be due to the presence of acetate, assigning the 1540 $cm^{-1}$ band to the $COO^-$ asymmetric stretching vibrations, and the 1390 $cm^{-1}$ band to the $COO^-$ symmetric stretching vibrations. Band at 1635 $cm^{-1}$ was assigned to the groups C–O (de Diego-Díaz et al., 2019). As can be seen in Fig. 1d, the increase in the generation of acetate (Eq. 1) occurred from day 11 until day 19, and after a plateau was observed.

The production of biogas was enhanced when the solubilization of acetate generated by the partial breakage of bonds in the fibers was possible, causing an important drop in the pH values; these phenomena were mainly observed until the day 14 (Fig. 1a–c). The highest values of acetate detected in the fibers which remained without solubilizing were observed from day 19 (Fig. 1d); at these periods, the production of biogas reduced drastically (Fig. 1a).

Fig. 3a shows the evolution of CODs in the reactors. During the first days, a slight increase was recorded due to the solubilization of organic matter in the hydrolysis and acidogenesis stages. However, in the case of L4, it solubilized until day 30, detecting a great difference with other reactors. This result coincided with the highest production of biogas of reactor L4 (Fig. 1a and b). In the case of L2, C2, C4, J2, J4, the solubilization took place during the first 19 days, when the production of biogas enhanced. The trend in DOC was similar to that registered in CODs (Fig. 3a and b). Again, these results indicated that the production of biogas was mainly produced in the first stages (until day 19). In general, higher DOC and CODs were measured for C2, L2 and J2. As well, the maximum methane yields were obtained in the reactors C2, L2 and J2 (Table 2).

The signal at 1335 $cm^{-1}$ was assigned to –OH in plane bending vibration and that at 1314 $cm^{-1}$ to the $CH_2$ wagging vibration (Colom et al., 2003). In Fig. 3c it was depicted this ratio (Eq. 2), which increased as the process progressed, therefore increasing the content of amorphous cellulose I (Colom et al., 2003). This behaviour was more significant from the day 19 of the process. As they were degraded the two IR signals evolved into a single band at 1305 $cm^{-1}$, mainly at day 40 (Fig. 2).

The crystallinity index (CrI) results obtained by XRD (Eq. 5) agreed with the data of amorphous content obtained by IR. In this sense, the highest values of CrI for C4, L4 and L2 occurred at 19 days, which matched with the minor values of amorphous content observed by IR. There was a marked decrease in the CrI of cotton, linen and jute from day 19 to day 40 (Fig. 3d and Table S2 – Supplementary material). The XRD diffractograms of the cellulose-based fibers at 0, 19 and 40 days are shown in Fig. S2-Supplementary material. Peaks at ca. $2\theta = 22.3°$ corresponded to the (200) plane, considered as the crystalline phase whilst that at ca. $2\theta = 16.3°$ was assigned to the amorphous phase.

Considering the linear regression on the data to estimate the CrI changes velocity (Table S3-supplementary material), it can be observed that J4 and J2 showed a faster decrease of the CrI (−0.47; −0.45 CrI/

**Table 2**
TOC and CODs consumptions; biogas and methane productions and yields in AD of different textile fabrics.

| Consumption/Production | | | | | | | | | | | | |
|---|---|---|---|---|---|---|---|---|---|---|---|---|
| | B | C4 | C2 | L4 | L2 | J4 | J2 | S2 | S1 | W2 | W1 | P2 | P1 |
| $TOC_{consumed}$ (mg/L) | 4.89 ±0.18 | 29.34 ±1.19 | 29.16 ±1.18 | – | 9.39 ±0.38 | 25.50 ±1.12 | 72.40 ±3.18 | 87.64 ±4.23 | 212.23 ±9.18 | 144.20 ±6.98 | 138.83 ±5.55 | 7.34 ±0.30 | 8.80 ±0.45 |
| $CODs_{consumed}$ ($mgO_2$/L) | 9.42 ±0.38 | 113.3 ±4.55 | 70.05 ±2.89 | – | 112.27 ±4.50 | 223.52 ±8.99 | 216.65 ±9.18 | 306.27 ±15.18 | 331.81 ±13.27 | 220.31 ±8.88 | 174.39 ±6.98 | 14.13 ±0.60 | 16.96 ±0.70 |
| Biogas (L) | 0.56 ±0.11 | 2.25 ±0.10 | 8.36 ±0.38 | 12.90 ±0.62 | 7.20 ±0.30 | 3.12 ±0.15 | 7.99 ±0.35 | 10.10 ±0.50 | 11.67 ±0.55 | 0.72 ±0.10 | 4.78 ±0.19 | 0.62 ±0.10 | 1.39 ±0.08 |
| Total methane (L) | 0.43 ±0.09 | 1.70 ±0.08 | 6.29 ±0.35 | 9.68 ±0.38 | 5.35 ±0.22 | 2.34 ±0.18 | 5.96 ±0.28 | 7.51 ±0.58 | 8.72 ±0.36 | 0.53 ±0.09 | 3.55 ±0.18 | 0.46 ±0.10 | 1.02 ±0.08 |
| Methane (%) | 76.50 ± 0.18 | 75.63 ± 0.65 | 75.32 ± 2.46 | 75.06 ± 3.76 | 74.34 ± 1.99 | 75.08 ± 0.91 | 74.67 ± 2.37 | 74.13 ± 0.11 | 74.20 ± 1.25 | 74.35 ± 2.78 | 74.69 ± 3.20 | 75.20 ± 0.20 | 73.10 ± 0.40 |
| Yields | B | C4 | C2 | L4 | L2 | J4 | J2 | S2 | S1 | W2 | W1 | P2 | P1 |
| $Methane/TOC_{consumed}$ (mL/g) | 29.20 ±1.35 | 19.33 ±0.87 | 71.94 ±3.23 | – | 189.87 ±8.51 | 30.57 ±1.39 | 27.45 ±1.26 | 28.56 ±1.30 | 13.69 ±0.80 | 1.23 0.08 | 8.52 ±0.48 | 21.02 ±1.10 | 38.63 ±1.86 |
| $Methane/CODs_{consumed}$ (mL/mg) | 15.16 ±0.75 | 5.01 ±0.28 | 29.95 ±1.35 | – | 15.88 ±0.71 | 3.49 ±0.21 | 9.17 ±0.51 | 8.17 ±0.41 | 8.76 ±0.43 | 0.80 ±0.06 | 6.78 ±0.41 | 10.91 0.51 | 20.05 ±0.95 |
| Methane/VS (L/kg) | – | 14.25 ±0.71 | 105.41 ±4.84 | 81.59 ±3.68 | 90.13 ±4.13 | 19.65 ±0.89 | 100.17 ±4.55 | 125.41 ±5.84 | 291.11 ±13.10 | 9.13 ±0.54 | 122.14 ±5.60 | 256.94 ±11.56 | 1133.33 ±49.00 |

days) comparing to C4 with −0.26 CrI/days. This can be related with the highest values of the amorphous content in this fabric.

The fiber textiles with the highest values of amorphous content corresponded to J2 and J4 (Fig. 3c) and consequently showed the minor crystallinity indexes (Fig. 3d and Table S2 – Supplementary material). On the contrary, the minor values in amorphicity were observed for both C2 and C4 (Fig. 3c), and also the highest values for CrI (Fig. 3d and Table S2 – Supplementary material). Cotton is considered as the purest form of cellulose in nature (Hsieh, 2007), having the highest values of cellulose compounds (ca. 90%) whilst jute usually shows a composition with cellulose ranging between 55% and 70% (Hsieh, 2007; Duan et al., 2017). The removal of non-cellulosic materials provided a rapid increase in relative crystallinity (Duan et al., 2017). Accordingly, in our study the highest crystallinity values were found when the composition of non-cellulosic materials (hemicellulose, lignin, pectin) was the minor as occurs for cotton.

The main mass losses corresponding to decomposition of cellulose within cotton, linen and jute occurred around 360 °C (Table 3 and Fig. S3-Supplementary material). As can be seen in Table S2 – Supplementary material, the fibers underwent a sudden change in temperature from day 19, so decomposition took place at much lower temperatures. The maxima of DTG were seen lower due to changes in crystallinity (Pérez-Rodríguez et al., 2018).

The degradation velocity (Table S4-Supplementary material) showed that the effect of the temperature in the cotton was more accentuated, since the slope was higher (−1.18 for C4; −1.10 °C/days for C2) comparing to Jute (−0.82 for J4; −0.65 °C/days for J2).

From the morphological point of view, C2, L2 and J2 at day 19 were seen more frayed than C4, L4 and J4, respectively (Fig. 4). This result was in line with those from both CrI (Fig. 3d) and amorphous content (Fig. 3c). Likewise, lower L* values were obtained in the fabrics submerged in the reactors with lower TS (C2, L2 and J2); decrease in values was clearly observed through the degradation processes (Table S5 – Supplementary material). Yellowing occurred in all fabrics over the days, higher in the case of the cotton (b* values from −6.57 to 18.22 for C4 and from 5.49 to 24.94 for C2).

### 3.2. Protein-based fabrics

As seen in Fig. 5a and b, the highest production of biogas for silk and wool occurred at 7 and 3 days respectively; this period corresponded to the hydrolytic and the first steps of the acidogenic stage (Fig. 5c). Therefore, the maxima biogas values concerning the protein-based fibers occurred at lower days compared with those found for the cellulose-based fibers (Fig. 1a and b). In all the protein-based fabrics studied, the methane composition was located in the range 74.1–74.7 ± 3.2% (Table 2). The higher values of biogas production were found when the concentration of solid fibers was minor (S1, W1). S1 showed the highest value of daily biogas production, ca. 1.0 L, at day 7 (Fig. 5a). The production of biogas was produced since proteins were broken down to amino acids, solubilized in a few days and quickly passed to be digested by microorganisms. A decrease in biogas production from day 7 was observed. Moreover, the minimum pH value was obtained at day 3 for both silk and wool (Fig. 5c), so it took only a few days for the hydrolytic and acidogenic phases to occur (Jeihanipour et al., 2013; Deublein and Steinhauser, 2008). The solubilization of the organic matter was produced at first stages, reaching the highest values at the first days and then, reducing or maintaining those (Fig. 5d and e). Therefore, no increase in CODs and DOC was observed through the process (Deublein and Steinhauser, 2008). In fact, the consumption of CODs and DOC in the liquid had led to the increment of biogas from the textile waste. The maximum methane yields were recorded in S2 and S1 compared to wool (Table 2).

The increase in amino acid content was clearly observed in silk by the presence of bands that appeared at 1002 and 985 $cm^{-1}$, corresponding to the gly-gly and gly-ala sequences respectively (Fig. 6a and

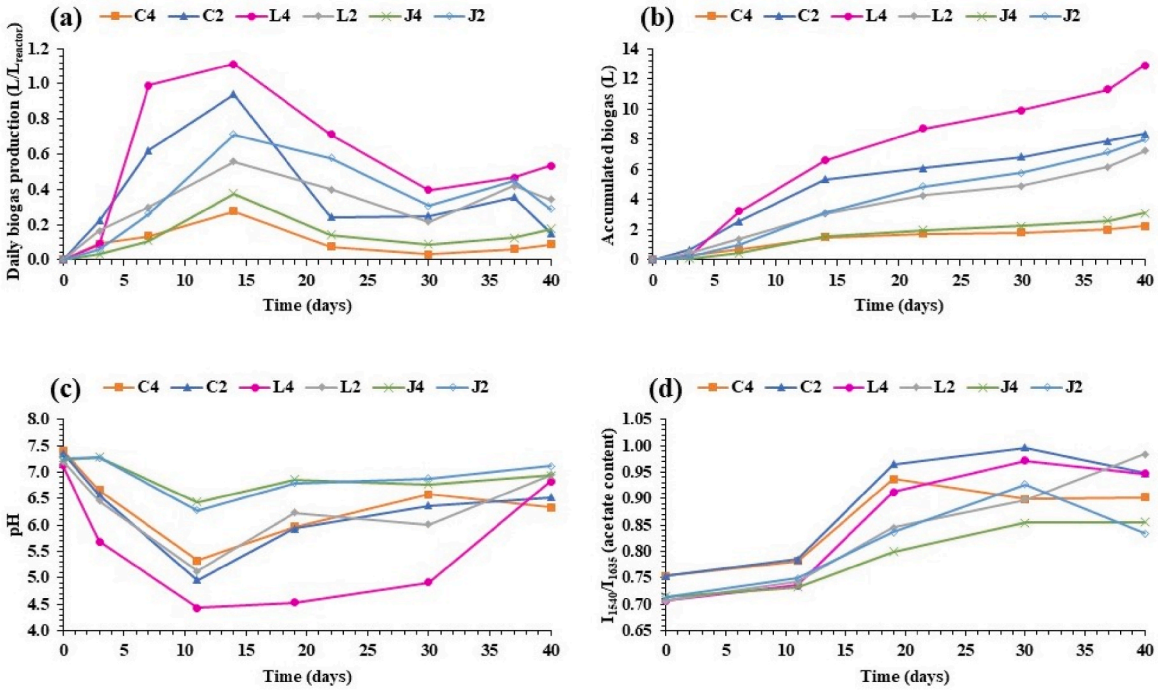


**Fig. 1.** (a) Daily biogas production in the reactors (L/Lreactor); (b) Accumulated biogas (L); (c) pH in the reactors; (d) Acetate content (using Eq. 1).

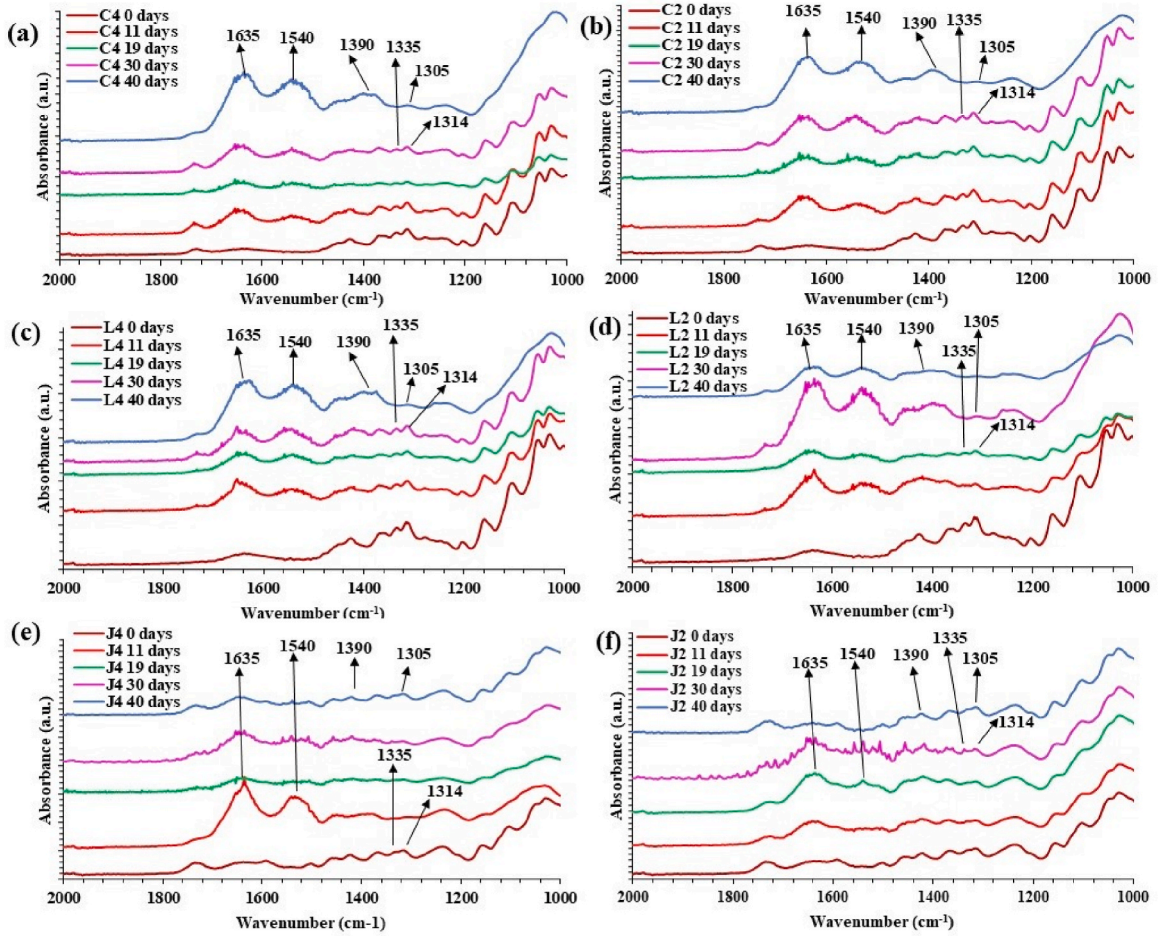


**Fig. 2.** Infrared spectra corresponding to: (a) cotton 4% (C4); (b) cotton 2% (C2); (c) linen 4% (L4); (d) linen (2%) (L2); (e) jute (4%) (J4); (f) jute (2%) (J2), at different days.

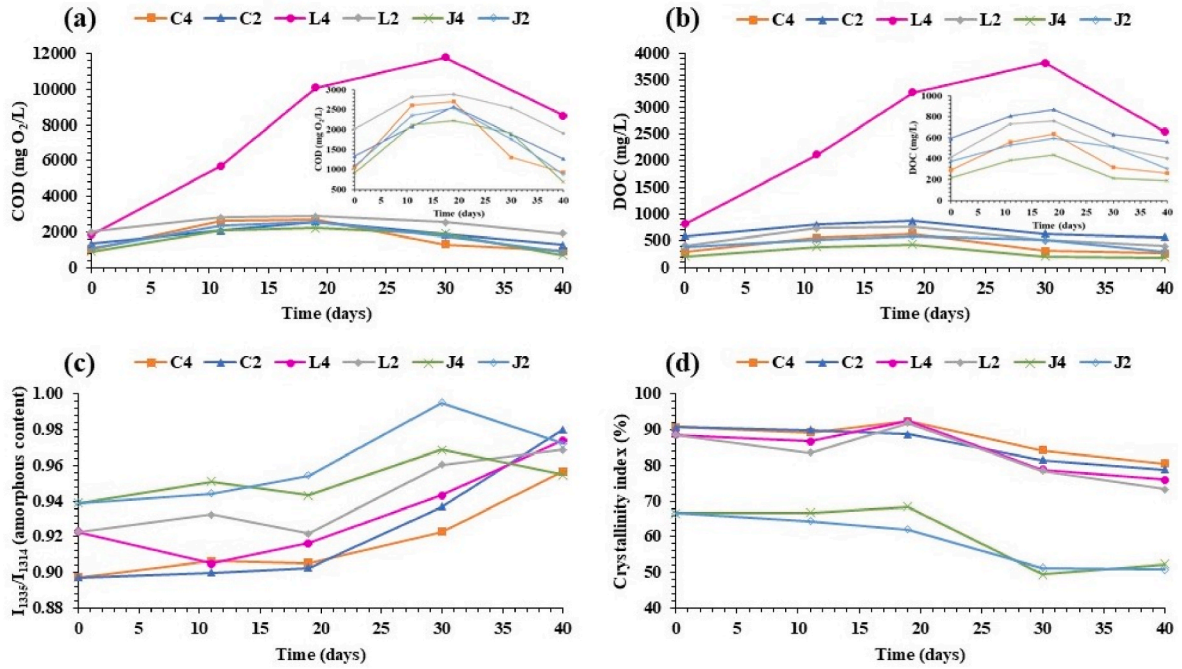


**Fig. 3.** (a) CODs in the reactors (mg $O_2$/L); (b) DOC in the reactors (mg/L); (c) Amorphous content (using Eq. 2); (d) Crystallinity index (using Eq. 5).

b). In the silk, the fibroin has a high crystallinity index due to the arranged β-sheets, showing the sericin a more random structure (Zang and Wyeth, 2010; Aksakal, 2016). The band at 3284 $cm^{-1}$ was assigned to the N–H stretching vibration of the amide A group (Aksakal, 2016). The ratio of intensities bands (Eq. 3) largely increased until day 19, especially the samples with the minor concentration, S1 in this case (Fig. 7a). The higher production of biogas also happened for S1 (Fig. 5a and b) thanks to the easier production of amino acids and biodegradation by microorganisms, which was mainly produced until day 14. Also, the degree of degradation of silk fibers was studied by relating the intensities of the bands at 1615 and 1655 $cm^{-1}$ (Eq. 4 and Fig. 7b), which corresponded to the crystalline β-sheets and the random coil arrangement respectively (Aksakal, 2016; Baimark et al., 2010). As can be seen in Fig. 7b, the crystallinity index decreased rapidly in the first days of the process due to the easier degradation of the proteins as they were in amorphous or randomly form.

The peak of loss of mass of silk fibers occurred around 320 °C (Table 4 and Fig. S3-Supplementary material), which corresponded to the breaking of peptide bonds in addition to the decomposition of the groups found in the side chains of amino acid residues (Duan et al., 2017). The temperatures decreased, especially for the S1 samples (Table 4).

As for the wool, amide I, II and III bonds correspond to the characteristic peptide bonds of the keratin protein found in this fiber. The wavenumber and absorbance intensity changes observed in the amide signals were attributed to modifications in the keratin conformations, mainly in helical (α-keratin) or rectal (β-keratin) forms (Wojciechowska et al., 1999). The peak at ca. 1626 $cm^{-1}$ was assigned to Amide I, connected with $\nu$ (C═O) vibration, and that at 1516 $cm^{-1}$ to Amide II, connected with deformating δ (N–H) and stretching $\nu$ (C–N) vibrations (Fig. 6). Amide III was related with bands at 1217 and 1244 $cm^{-1}$ (Wojciechowska et al., 1999). Following Eq. 4, this one increased until day 11 as shown in Fig. 7b. An increase in this ratio was the result of the higher hydrolysis of peptide bonds, producing the largest increase during the first days of the process, coinciding with the data obtained by using the other techniques. From day 11, a plateau was observed (Fig. 7b). The hydrolysis of the wool in the AD reactor was clearly higher when the solid amount was minor (W1 compared with W2). This significant increase in peptide bond hydrolysis during the first days correlated with the data obtained in thermal analysis, where a drastic decrease in decomposition temperature occurred in the first eleven days (Table 4 and Fig. S3-supplementary material). The mass loss signal located at 345 °C corresponded to the denaturation of the polypeptide chain in keratin. As of day 11, the decomposition temperature also dropped slightly.

In the case of protein-based fibers, the degradation velocity, using a linear regression (Table S4-Supplementary material) showed that the effect of temperature in silk was lower (−0.08 for S2; −0.26 °C/days for S1) compared to wool (−0.84 for W2; −0.64 °C/days for W1).

Major degradation was visually detected for S1 and W1 (Fig. 4). Likewise, in these samples (S1 and W1) a tendency to higher b* values were measured. The values of L* also decreased, especially for W1 (Table S5 – Supplementary material).

### 3.3. Synthetic fabric

Fig. 8 shows the different biomethanization parameters measured for polyester fibers at different concentrations (P1 and P2). The biogas values obtained were very low in comparison with those obtained for cellulosic and protein-based fabrics (Fig. 1a, b, 5a and 5b). Maxima of 0.09 L were found for P1 and P2 in day 14, whilst the maxima for cellulose-based fibers were ranging 0.2–1.1 L/day and those for protein-based fibers between 0.1 and 1.0 L/day. As for the pH, a slight decrease until day 11 was observed, after which it raised slightly (Fig. 8c). In addition, a slight increase in CODs was observed in the first 19 days (Fig. 8d). In contrast, an increase in DOC was not observed (Fig. 8e).

**Table 3**
Temperatures of maximum mass loss rate (in °C) for cellulose-based fabrics according to time of anaerobic biodegradation (days).

| | C4 | C2 | L4 | L2 | J4 | J2 |
|---|---|---|---|---|---|---|
| 0 days | 355.10 | 355.10 | 359.66 | 359.66 | 366.70 | 366.70 |
| 11 days | 353.58 | 352.88 | 349.45 | 355.38 | 367.51 | 358.30 |
| 19 days | 344.73 | 354.31 | 326.75 | 353.17 | 349.19 | 351.51 |
| 30 days | 329.18 | 326.56 | 320.74 | 325.27 | 339.64 | 345.35 |
| 40 days | 309.07 | 314.16 | 313.28 | 317.25 | 339.49 | 340.86 |

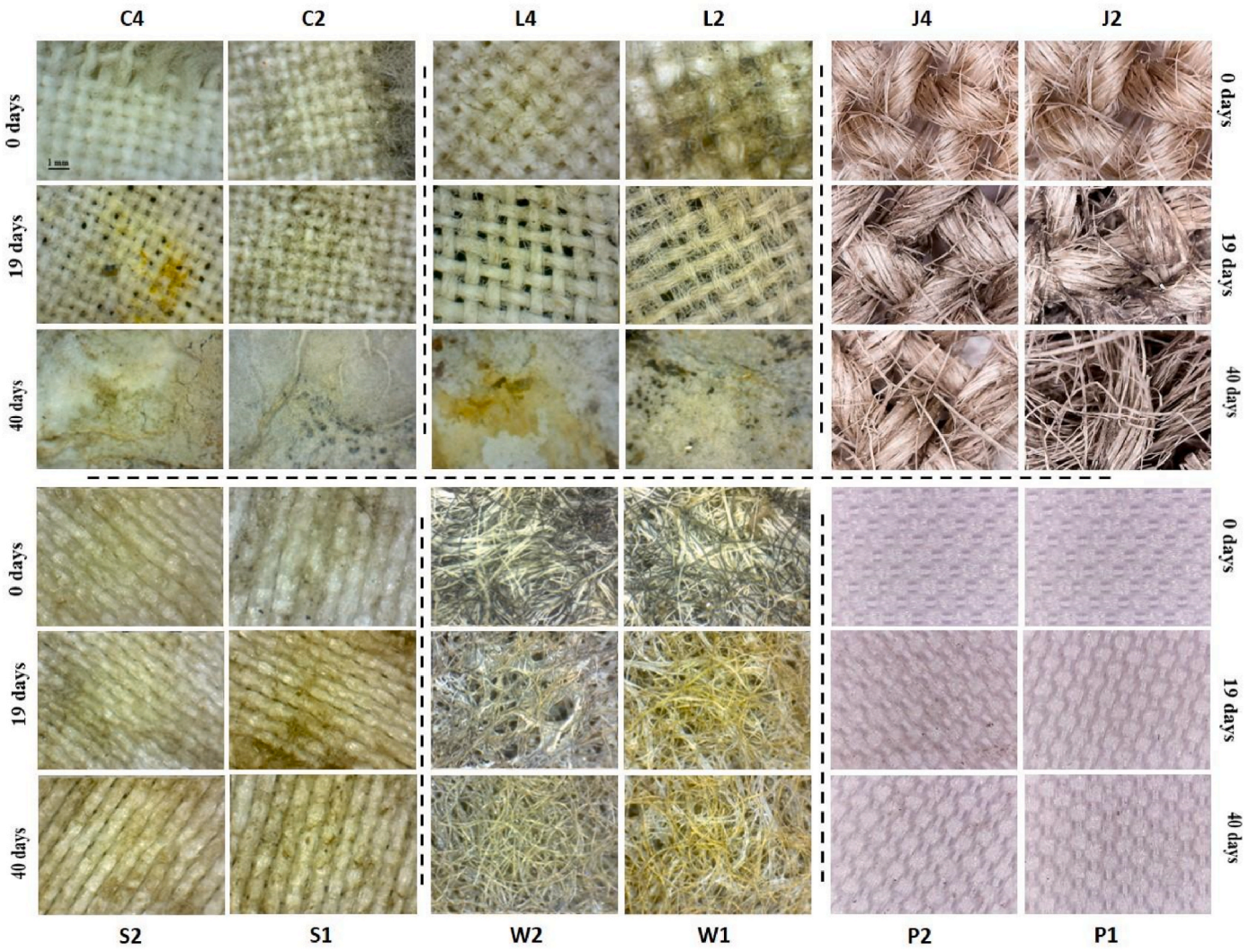


**Fig. 4.** Micrographs corresponding to the fibers (C4, C2, L4, L2, J4, J2, S2, S1, W2, W1, P2 and P2) after the biodegradation processes at 0, 19 and 40 days.

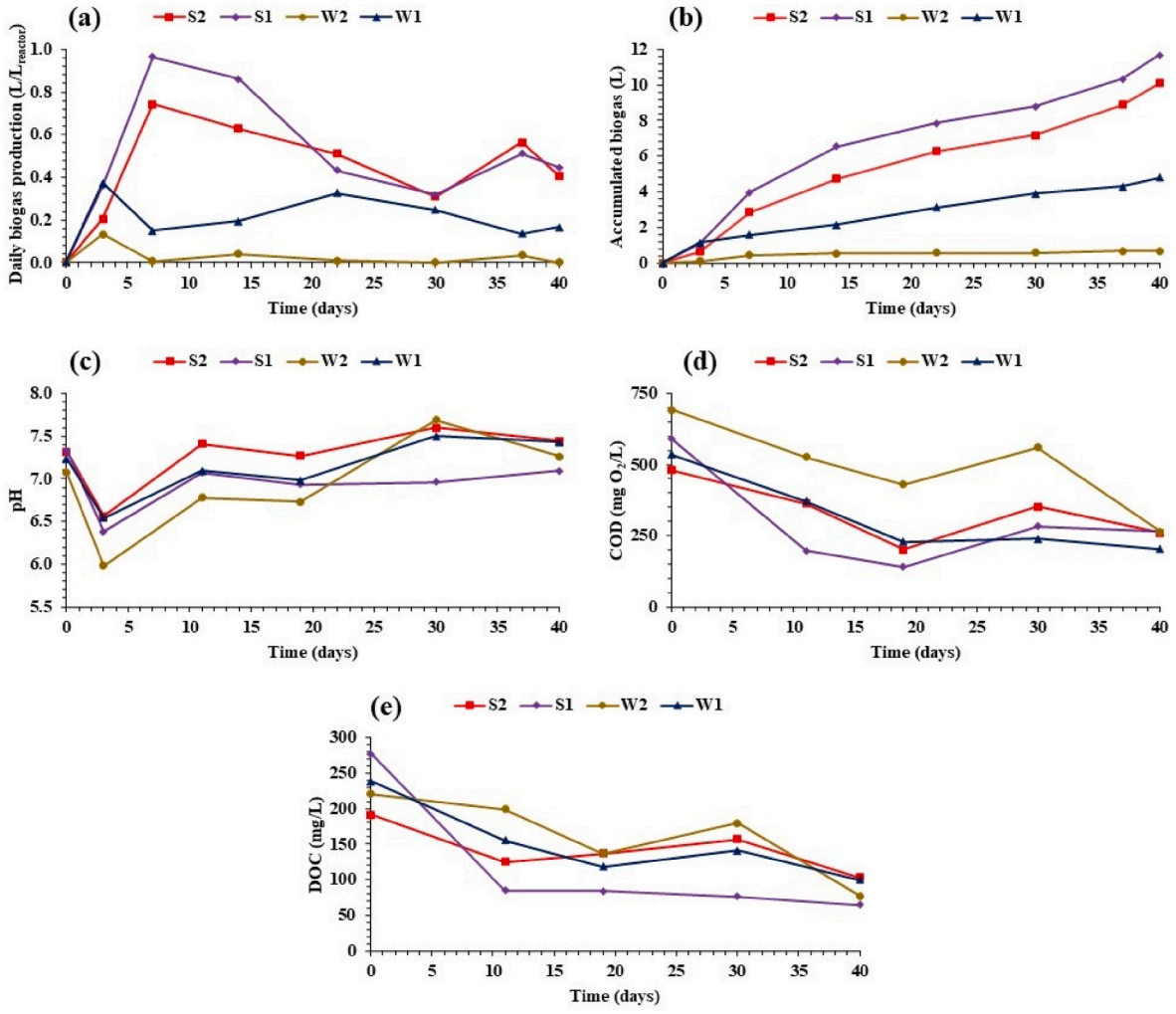


**Fig. 5.** (a) Daily biogas production in the reactors (L/Lreactor); (b) Accumulated biogas (L); (c) pH in the reactors; (d) CODs in the reactors (mg $O_2$/L); (e) DOC in the reactors (mg/L).

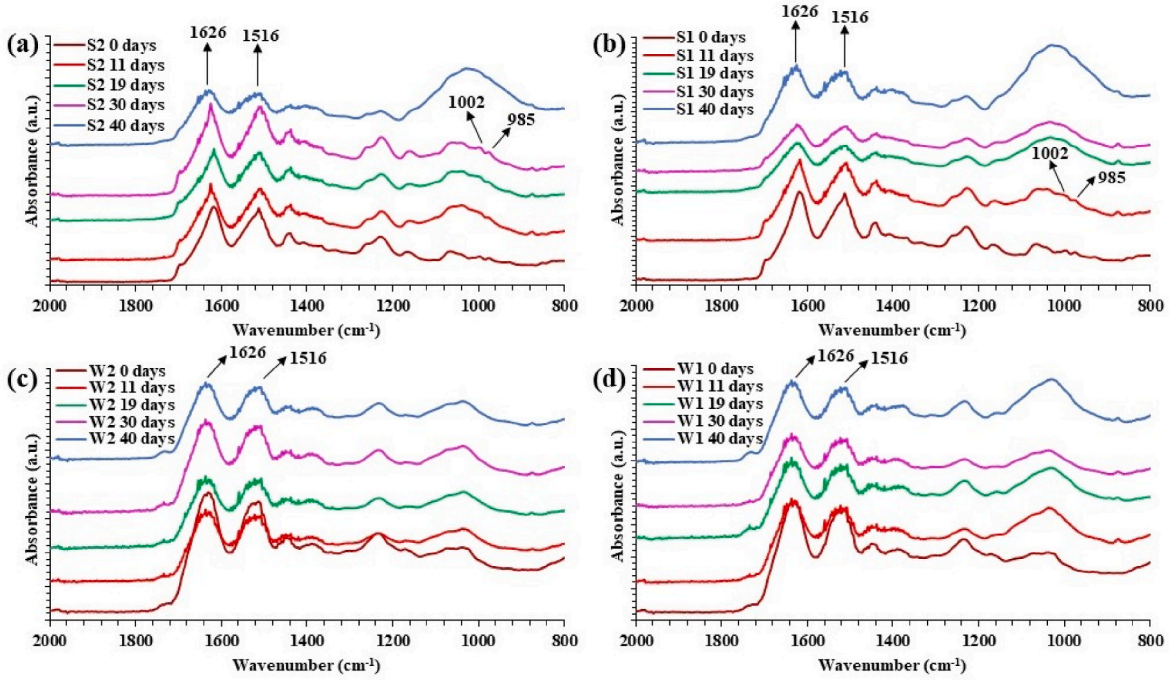


**Fig. 6.** Infrared spectra corresponding to: (a) silk 2% (S2); (b) silk 1% (S1); (c) wool 2% (W2); (d) wool 1% (W1), at different days.

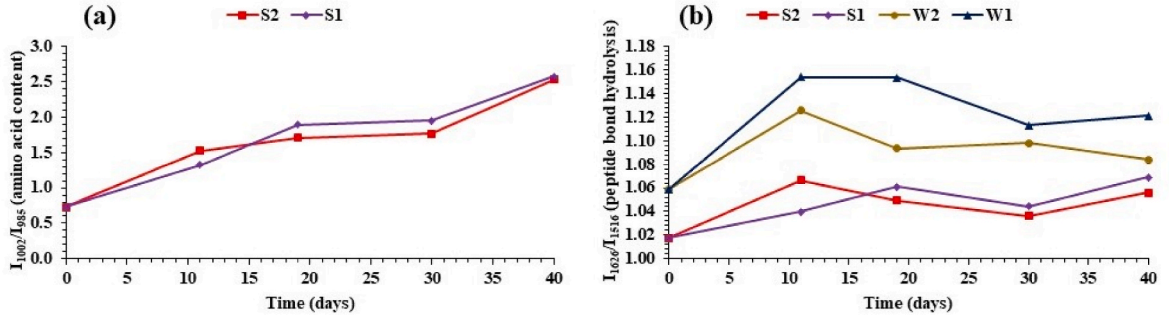


**Fig. 7.** (a) Amino acid content of the silk fibers (using Eq. 3); (b) Degree of degradation of the silk and wool fibers due to the peptide bond hydrolysis (using Eq. 4).

**Table 4**
Temperatures of maximum mass loss rate (in °C) for protein fibers according to time of anaerobic biodegradation (days).

| | S2 | S1 | W2 | W1 |
|---|---|---|---|---|
| 0 days | 323.27 | 323.27 | 345.43 | 345.43 |
| 11 days | 319.61 | 322.54 | 320.78 | 319.46 |
| 19 days | 320.98 | 321.75 | 315.39 | 314.74 |
| 30 days | 319.99 | 317.76 | 308.05 | 313.16 |
| 40 days | 319.38 | 312.84 | 310.08 | 316.95 |

The stability of the polyester fibres was also demonstrated by using both IR and XRD techniques (Fig. S4-Supplementary material). Regarding the thermal analysis, polyester suffered a single mass loss at ca. 440 °C (Table 5 and Fig. S4-Supplementary material) due to depolymerization processes. A slight diminution in the DTG temperatures was detected in the first 11 days (from 440 °C to 432 °C for P2, and from 440 °C to 435 °C for P1), matching rather well with data of the maxima biogas production at the first days. From the types of fibers studied, the polyester was the one less affected by the temperature degradation, with a velocity of −0.20; −0.17 °C/days (Table S4-Supplementary material). The morphology of the fibres of polyester and colour were not significantly affected with the treatment (Fig. 4 and Table S5 – Supplementary material).

### 3.4. Kinetic analysis

The model fitted accurately all the experimental conditions, being the coefficient of determination $R^2$ ranged from 0.921 to 0.983, similar values to those reported in the literature (Table 6) (Juanga-Labayen and Yuan, 2021; Krungkaew et al., 2022; Ebrahimzade et al., 2022). The maximum methane yield, $y_m$, represents the methane production potential. The variation of specific methane yield potential was highest in the S1 (271.79 L/kgVSadded) compared to polyester (2% 0.48 and 1% 1.93 L/kgVSadded), highlighting the low biodegradation of synthetic fibers.

Lower results also were reported in natural fibers in W2, C4 and J4 with 8.22, 12.97 and 18.21 L/kgVSadded, respectively. In all cases, the higher concentration of total solids in the reactor is limiting the performance of AD. In the previous conditions: W1 133.04; C2 98.96, and J2 104.44 L/kgVSadded). Similar conclusions were obtained by Fernández-Rodríguez et al. (2010), and Juanga-Labayen and Yuan, 2021.

Similar trends were observed in the maximum methane production rate, $R_{max.}$. The highest value was found in S1 (11.32 L/kgVSadded.day respectively) and the lowest in polyester (Table 6). C4 reached 5.28 L/

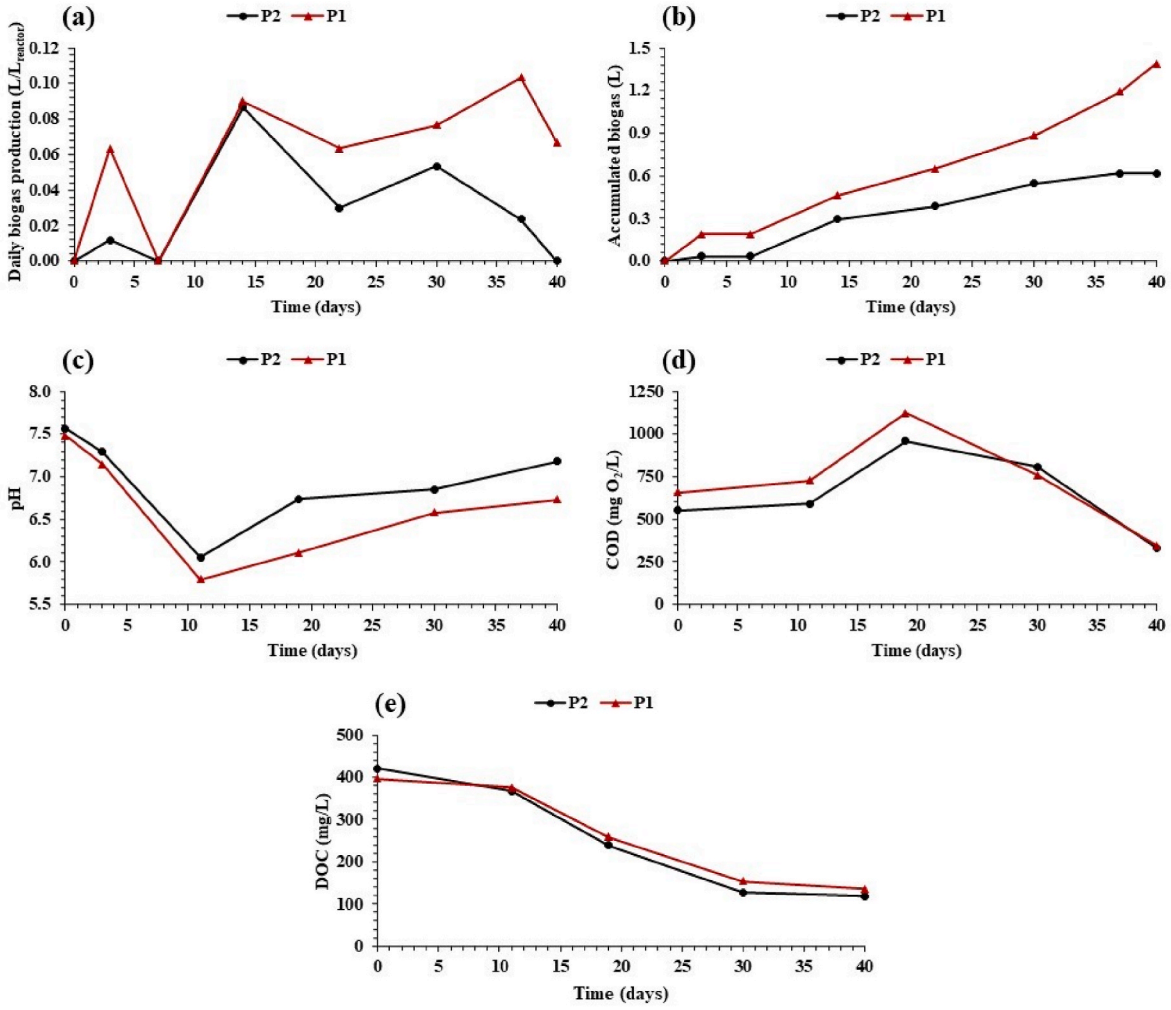


**Fig. 8.** (a) Daily biogas production in the reactors (L/Lreactor); (b) Accumulated biogas (L); (c) pH in the reactors; (d) CODs in the reactors (mg $O_2$/L); (e) DOC in the reactors (mg/L).

**Table 5**
Temperatures of maximum mass loss rate (in °C) for polyester fabrics according to time of anaerobic biodegradation (days).

| | P2 | P1 |
|---|---|---|
| 0 days | 440.38 | 440.38 |
| 11 days | 431.75 | 430.40 |
| 19 days | 430.78 | 430.79 |
| 30 days | 429.10 | 432.52 |
| 40 days | 432.03 | 430.94 |

kgVSadded.day, value in concordance to Juanga-Labayen and Yuan (2021), who reported 4.02 L/kgVSadded.day in AD of cotton waste. However, Ebrahimzade et al. (2022) informed 22 and 40 mL CH4/g.VS. day in AD of cellulosic starch-based bioplastic.

The minimum time to produce methane, the lag time, $\lambda$, was over 0 days in all the animal fibers. However, in the vegetal fibers, cotton and linen lasted 1.34–1.93 days and jute around 3.5 days. During the first moments of AD, the anaerobic microbiota scarcely produces methane from substrates based on a complex structure as lignocellulosic materials (Ziemiński and Kowalska-Wentel, 2015).

**Table 6**
Kinetic parameters of the modified Gompertz model for the BMP of natural and synthetic textile fibers.

| | Cotton 4% | | Cotton 2% | | Linen 4% | | Linen 2% | | Jute 4% | | Jute 2% | |
|---|---|---|---|---|---|---|---|---|---|---|---|---|
| $R_{max}$ (L/kg-$VS_{added}$ day) | 0.78 | ±0.14 | 5.28 | ±0.93 | 3.30 | ±0.59 | 2.71 | ±0.42 | 0.78 | ±0.17 | 3.50 | ±0.45 |
| $\lambda$ (days) | 1.42 | ±1.31 | 1.38 | ±1.45 | 1.93 | ±1.81 | 1.34 | ±2.12 | 3.07 | ±2.27 | 3.78 | ±1.56 |
| $y_m$ (L/kg-$VS_{added}$) | 12.97 | ±0.56 | 98.96 | ±4.83 | 77.21 | ±5.32 | 95.91 | ±13.02 | 18.21 | ±1.62 | 104.44 | ±9.00 |
| $R^2$ | 0.974 | | 0.973 | | 0.970 | | 0.969 | | 0.958 | | 0.983 | |
| | Wool 2% | | Wool 1% | | Silk 2% | | Silk 1% | | Polyester 2% | | Polyester 1% | |
| $R_{max}$ (L/kg-$VS_{added}$ day) | 0.76 | ±0.35 | 3.51 | ±0.57 | 3.97 | ±0.74 | 11.32 | ±2.40 | 0.02 | ±0.00 | 0.03 | ±0.00 |
| $\lambda$ (days) | −1.59 | ±2.35 | −2.48 | ±2.32 | 0.25 | ±2.36 | −0.04 | ±2.14 | 4.72 | ±1.71 | 4.64 | ±3.57 |
| $y_m$ (L/kg-$VS_{added}$) | 8.22 | ±0.62 | 133.04 | ±17.30 | 127.32 | ±15.50 | 271.79 | ±21.38 | 0.48 | ±0.03 | 1.93 | ±0.88 |
| $R^2$ | 0.921 | | 0.964 | | 0.959 | | 0.954 | | 0.980 | | 0.978 | |

## 4. Conclusions

For the cellulose-based fibers, the production of biogas was enhanced until day 14 thanks to the easier solubilization of acetate. The highest values of acetate detected in the fibers, which remain without solubilizing, were observed from day 19; at these periods, the production of biogas decreased drastically. The amorphicity of cotton, linen and jute decidedly increased from day 19. Except for linen, the highest generation of biogas and methane yield was produced for the samples with lower solid concentrations (C2, L2 and J2 showed the highest amorphous values and C4, L4 and J4 the highest crystallinity index). The maxima in the biogas production of the protein-based fibers occurred at lower days (day 7 for the silk and day 3 for the wool). The maximum methane yield was detected for the samples with minor solid amounts. The arrangement of the fibroin and keratin proteins was modified. Gompertz model fitted properly the experimental data ($R^2$ from 0.921 to 0.983), showing that the lag phase was almost 0 days in the animal fibers and around 2 days in the cellulose-based fibers. The maximum specific methane production rate was detected in silk with lower solid concentration, 1%, with 11.32 $L/kgVS_{added}.day$.

Based on the results, the anaerobic digestion of natural fabrics can carry out, since the process modified the structure of the fibers. Perhaps, the performance could be optimized applying new configurations like thermophilic temperature (55 °C), an extended residence time of fabrics in the reactors or, even, the application of pretreatment strategies (acid, basic or both chemical media).

## Credit author statement

JF-R and AD contributed to the study conception and design. Material preparation, data collection and analysis were performed by JA, CO, AD and JF-R. The first draft of the manuscript and the revised version were written by AD and JF-R.

## Declaration of competing interest

The authors declare that they have no known competing financial interests or personal relationships that could have appeared to influence the work reported in this paper.

## Data availability

Data will be made available on request.

## Acknowledgments

The authors thank Cristina Luzuriaga, Marta Yárnoz and Ibon Iribarren for their assistance.

## Appendix A. Supplementary data

Supplementary data to this article can be found online at https://doi.org/10.1016/j.jenvman.2023.118366.

## References

Aili Hamzah, F., Hamzah, M.H., Man, H.C., Jamali, N.S., Siajam, S.I., Ismail, M.H., 2021. Recent updates on the conversion of pineapple waste (ananas comosus) to value-added products, future perspectives and challenges. Agronomy 11 (11), 2221. https://doi.org/10.3390/agronomy11112221.

Aksakal, B., 2016. Temperature effect on the recovery process in stretched Bombyx mori silk fibers. Spectrochim. Acta 152, 629–636. https://doi.org/10.1016/j.saa.2015.01.105.

APHA/AWWA/WPCF, 2012. Standard Methods for the Examination of Water and Wastewater, twenty-second ed. American Public Health Association, Washington D. C.

Baimark, Y., Srisa-ard, M., Srihanam, P., 2010. Morphology and thermal stability of silk fibroin/starch blended microparticles. Express Polym. Lett. 4 (12), 781–789. https://doi.org/10.3144/expresspolymlett.2010.94.

Bhatia, S.K., Joo, H.-S., Yang, Y.-H., 2018. Biowaste-to-bioenergy using biological methods—a mini-review. Energy Convers. Manag. 177, 640–660. https://doi.org/10.1016/j.enconman.2018.09.090.

Binczarski, M.J., Malinowska, J.Z., Berlowska, J., Cieciura-Wloch, W., Borowski, S., Cieslak, M., Puchowicz, D., Witonska, I.A., 2022. Concept for the use of cotton waste hydrolysates in fermentation media for biofuel production. Energies 15 (8), 2856. https://doi.org/10.3390/en15082856.

Colom, X., Carrillo, F., Nogués, F., Garriga, P., 2003. Structural analysis of photodegraded wood by means of FTIR spectroscopy. Polym. Degrad. Stabil. 80 (3), 543–549. https://doi.org/10.1016/S0141-3910(03)00051-X.

De Diego-Díaz, B., Duran, A., Álvarez-García, M.R., Fernández-Rodríguez, J., 2019. New trends in physicochemical characterization of solid lignocellulosic waste in anaerobic digestion. Fuel 245, 240–246. https://doi.org/10.1016/j.fuel.2019.02.051.

Deublein, D., Steinhauser, A., 2008. Biogas from Waste and Renewable Resources: an Introduction, first ed. WILEY-VCH Verlag GmbH & Co. KGaA, Weinheim. https://doi.org/10.1002/9783527621705.

Duan, L., Yu, W., Li, Z., 2017. Analysis of structural changes in jute fibers after peracetic acid treatment. J. Eng. Fibers Fabrics 12 (1), 33–42. https://doi.org/10.1177/155892501701200104.

Ebrahimzade, M., Ebrahimi-Nik, Rohani, A., Tedesco, S., 2022. Towards monitoring biodegradation of starch-based bioplastic in anaerobic condition: finding a proper kinetic model. Bioresour. Technol. 347, 126661 https://doi.org/10.1016/j.biortech.2021.126661.

Fernández-Rodríguez, J., Perez, M., Romero, L.I., 2010. Kinetics of mesophilic anaerobic digestion of the organic fraction of municipal solid waste: influence of initial total solid concentration. Bioresour. Technol. 101, 6322–6328. https://doi.org/10.1016/j.biortech.2010.03.046.

Fernández-Rodríguez, J., Pérez, M., Romero, L.I., 2013. Comparison of mesophilic and thermophilic dry anaerobic digestion of OFMSW: kinetic analysis. Chem. Eng. J. 232, 59–64. https://doi.org/10.1016/j.cej.2013.07.066.

Ghasemian, M., Zilouei, H., Asadinezhad, A., 2016. Enhanced biogas and biohydrogen production from cotton plant wastes using alkaline pretreatment. Energy Fuel. 30 (12), 10484–104893. https://doi.org/10.1021/acs.energyfuels.6b01999.

Hasanzadeh, E., Mirmohamadsadeghi, S., Karimi, K., 2018. Enhancing energy production from waste textile by hydrolysis of synthetic parts. Fuel 218, 41–48. https://doi.org/10.1016/j.fuel.2018.01.035.

Holliger, M., Alves, D., Andrade, I., Angelidaki, S., Astals, U., Baier, et al., 2016. Towards a standardization of biomethane potential tests. Water Sci. Technol. 74 (11), 2515–2522. https://doi.org/10.2166/wst.2016.336.

Hsieh, Y.L., 2007. Chemical structure and properties of cotton. In: Gordon, S., Hsieh, Y.L. (Eds.), Cotton: Science and Technology, first ed. Woodhead Publishing Limited, Cambridge, pp. 3–34.

Isci, A., Demirer, G.N., 2007. Biogas production potential from cotton wastes. Renew. Energy 32 (5), 750–757. https://doi.org/10.1016/j.renene.2006.03.018.

Jeihanipour, A., Aslanzadeh, S., Rajendran, K., Balasubramanian, G., Taherzadeh, M.J., 2013. High-rate biogas production from waste textiles using a two-stage process. Renew. Energy 52, 128–135. https://doi.org/10.1016/j.renene.2012.10.042.

Juanga-Labayen, J., Yanac, K., Yuan, Q., 2020. Effect of substrate-to-inoculum ratio on anaerobic digestion of treated and untreated cotton textile waste. Int. J. Environ. Sci. Technol. 18, 287–296. https://doi.org/10.1007/s13762-020-02831-9.

Juanga-Labayen, J., Yuan, Q., 2021. Making biodegradable seedling pots from textile and paper waste—Part B: development and evaluation of seedling pots. Int. J. Environ. Res. Publ. Health 18 (14), 7609. https://doi.org/10.3390/ijerph18147609.

Johnravindar, D., Kumar, R., Luo, L., Jun, Z., Manu, M.K., Wang, H., Wong, J.W.C., 2023. Influence of inoculum-to-substrate ratio on biogas enhancement during biochar-assisted co-digestion of food waste and sludge. Environ. Technol. 2, 1–13. https://doi.org/10.1080/09593330.2022.2161949.

Kothari, R., Pandey, A.K., Kumar, S., Tyagi, V.V., Tyagi, S.G., 2014. Different aspects of dry anaerobic digestion for bio-energy: an overview. Renew. Sustain. Energy Rev. 39, 174–195. https://doi.org/10.1016/j.rser.2014.07.011.

Krungkaew, S., Hülsemann, B., Kingphadung, K., Mahayothee, B., Oechsner, H., Müller, J., 2022. Methane production of banana plant: yield, kinetics and prediction models influenced by morphological parts, cultivars and ripening stages. Bioresour. Technol. 360, 127640 https://doi.org/10.1016/j.biortech.2022.127640.

Kuzmanova, E., Zhelev, N., Akunna, J.C., 2018. Effect of liquid nitrogen pre-treatment on various types of wool waste fibres for biogas production. Heliyon 4 (5), e00619. https://doi.org/10.1016/j.heliyon.2018.e00619.

Lee, H., Behera, S.K., Kim, J.W., Park, H.S., 2009. Methane production potential of leachate generated from Korean food waste recycling facilities: a lab-scale study. Waste Manag. 29 (2), 876–882. https://doi.org/10.1016/j.wasman.2008.06.033.

Li, W., Lou, Y., Fang, A.R., Feng, K., Xing, D.F., 2020. Potassium permanganate (KMnO4)/sodium sulfite (Na2SO3) rapidly disintegrates waste activated sludge by reactive Mn(III) species and shapes microbial community structure. Chem. Eng. J. 394, 124920 https://doi.org/10.1016/j.cej.2020.124920.

Moazzem, S., Wang, L., Daver, F., Crossin, E., 2021. Environmental impact of discarded apparel landfilling and recycling. Resour. Conserv. Recycl. 166, 105338 https://doi.org/10.1016/j.resconrec.2020.105338.

Morton, W.E., Hearle, J.W.S., 2008. Physical Properties of Textile Fibres, fourth ed. Woodhead Publishing Limited, Cambridge, p. 776. 2008.

Olguin, C., Azcona, J., Fernández-Rodríguez, J., Durán, A., 2022. Acid and alkali chemical treatments on synthetic and natural cellulosic, fibroin and keratin-based fabrics: study of the structural changes. J. Text. Inst. https://doi.org/10.1080/00405000.2022.2144663.

Peng, J., Abomohra, A., Elsayed, M., Zhang, X., Fan, Q., Ai, P., 2019. Compositional changes of rice straw fibers after pretreatment with diluted acetic acid: towards

enhanced biomethane production. J. Clean. Prod. 230, 775–782. https://doi.org/10.1016/j.jclepro.2019.05.155.
Pérez-Rodríguez, J.L., Pérez-Maqueda, R., Franquelo, M.L., Duran, A., 2018. Study of the thermal decomposition of historical metal threads. J. Therm. Anal. Calorim. 134, 15–22. https://doi.org/10.1007/s10973-017-6924-x.
Ramawat, K.G., Ahuja, M.R. (Eds.), 2016. Fiber Plants: Biology, Biotechnology and Applications. Springer International Publishing AG, Switzerland, p. 258.
Ran, Y., Elsayed, M., Eraky, M., Dianlong, W., Ai, P., 2022. Sequential Production of Bioethane and Biomethanol through the Whole Biorefining of Rice Straw: Analysis of Structural Properties and Mass Balance. Biomass Conv. Biorefinery. https://doi.org/10.1007/s13399-022-02548-4.
Sasaki, K., Sasaki, D., Tsuge, Y., Morita, M., Kondo, A., 2021. Enhanced methane production from cellulose using a two-stage process involving a bioelectrochemical system and a fixed film reactor. Biotechnol. for Biofuels and Bioproducts 14, 7. https://doi.org/10.1186/s13068-020-01866-x.
Thomas, C.M., 2010. Stereocontrolled ring-opening polymerization of cyclic esters: synthesis of new polyester microstructures. Chem. Soc. Rev. 39, 165–173. https://DOI:10.1039/B810065A.
Villain, M., Bourven, I., Guibaud, G., Marrot, B., 2014. Impact of synthetic or real urban wastewater on membrane bioreactor (MBR) performances and membrane fouling under stable conditions. Bioresour. Technol. 155, 235–244. https://doi.org/10.1016/j.biortech.2013.12.063.
Wang, X., Shen, J., Chen, Z., Zhao, X., Xu, H., 2016. Removal of pharmaceuticals from synthetic wastewater in an aerobic granular sludge membrane bioreactor and determination of the bioreactor microbial diversity. Appl. Microbiol. Biotechnol. 100 (18), 8213–8223. https://doi.org/10.1007/s00253-016-7577-6.
Wojciechowska, E., Wlochowicz, A., Weselucha-Birczynska, A., 1999. Application of Fourier-transform infrared and Raman spectroscopy to study degradation of wool fiber keratin. J. Mol. Struct. 511–512, 307–318. https://doi.org/10.1016/S0022-2860(99)00173-8.
Xia, T., Sun, E., Tang, W., Huang, H., Wu, G., Jin, X., 2018. Structural and thermal stability changes of rice straw fibers during anaerobic digestion. BioResour 13 (2), 3447–3461.
Yurtsever, A., Calimlioglu, B., Sahinkaya, E., 2017. Impact of SRT on the efficiency and microbial community of sequential anaerobic and aerobic membrane bioreactors for the treatment of textile industry wastewater. Chem. Eng. J. 314, 378–387. https://doi.org/10.1016/j.cej.2016.11.156.
Zang, X.M., Wyeth, P., 2010. Using FTIR spectroscopy to detect sericin on historic silk. Sci. China Chem. 53 (3), 626–631. https://doi.org/10.1007/s11426-010-0050-y.
Zhang, H., Ning, Z., Khalid, H., Zhang, R., Liu, G., Chen, C., 2018. Enhancement of methane production from Cotton Stalk using different pretreatment techniques. Sci. Rep. 8, 3463. https://doi.org/10.1038/s41598-018-21413-x.
Ziemiński, K., Kowalska-Wentel, M., 2015. Effect of enzymatic pretreatment on anaerobic co-digestion of sugar beet pulp silage and vinasse. Bioresour. Technol. 180, 274–280. https://doi.org/10.1016/j.biortech.2014.12.035.
Zwietering, M.H., Jongenburger, I., Rombouts, F.M., Van 't Riet, K., 1990. Modeling of the bacterial growth curve. Appl. Environ. Microbiol. 56 (6), 1875–1881. https://doi: 10.1128/aem.56.6.1875-1881.1990.